RESEARCH ARTICLE

Mechanical and signaling mechanisms that guide pre-implantation embryo movement

Diana Flores[1,3], Manoj Madhavan[2,3], Savannah Wright[3] and Ripla Arora[1,2,3,*]

ABSTRACT

How a mammalian embryo determines and arrives at its attachment site has been studied for decades, but our understanding of this process is far from complete. Using confocal imaging and image analysis, we evaluate embryo location along the longitudinal oviductal-cervical axis of murine uteri. Our analysis reveals three distinct pre-implantation phases: embryo entry, unidirectional movement of embryo clusters and bidirectional scattering and spacing of embryos. We show that unidirectional clustered movement is facilitated by a mechanical stimulus of the embryo and is regulated by adrenergic uterine smooth muscle contractions. Embryo scattering, on the other hand, depends on embryo-uterine communication reliant on the LPAR3 signaling pathway and is independent of adrenergic muscle contractions. Finally, we demonstrate that uterine implantation sites in mice are neither random nor predetermined but are guided by the number of embryos entering the uterine lumen. These studies have implications for understanding how embryo-uterine communication is key to determining an optimal implantation site necessary for the success of a pregnancy.

KEY WORDS: Murine embryo spacing, Embryo-uterine interactions, Implantation, Muscle contraction, LPAR3, Mouse

INTRODUCTION

In the biology of maternal-fetal interactions, one of the crucial steps is the communication of the early embryo with the uterine milieu to find a 'good' site for attachment. In addition, in multiparous species, embryos face a unique challenge of achieving adequate spacing to avoid competition for maternal resources. The mouse model serves as an excellent system to address both these questions in early mammalian pregnancy. Reproducible patterns of implantation, such as attachment near the fundus in humans, which are monotocous (single offspring) species (Bulletti and de Ziegler, 2005), and even distribution of embryos along the uterine length in rats and rabbits, which are polytocous (multiple offspring) species (Boving, 1956; O'Grady and Heald, 1969), suggest evolutionary mechanisms that have been selected to allow for these patterns.

In 1956, Boving suggested that embryo distribution at implantation reflects whether its location is acquired randomly due to diffusion and muscle contraction movements or due to a pre-determined stimulator-effector system (Boving, 1956). Quantitative analysis of embryo spacing has been performed in the rabbit model system (Boving, 1956) and in the rat (O'Grady and Heald, 1969). These studies suggested that embryo distribution is not random, implying that embryo-uterine and/or embryo-embryo interactions are crucial for determining implantation sites. In the rabbit, embryo distribution along the uterus was measured using two features: the distance of an individual blastocyst away from the oviductal-uterine junction and the relative distance between successive embryos. Embryo-embryo distance continuously increased over time, suggesting that embryos enter and move unidirectionally while separating, and achieve equal spacing only before implantation (Boving, 1956). In the rat, embryo distribution was analyzed after entry into the uterus until implantation. For location analysis, the uterus was cut into three segments of equal length, and the number of embryos was quantified by flushing each of these segments. All embryos are initially present in the rostral segment – closer to the oviduct. Over time, the embryos appear to distribute in the first and second segments and, eventually, along the horn evenly (Pusey et al., 1980). Such distribution suggests that in the rat, similar to the rabbit (Boving, 1956), embryos enter the uterine horn and move in a unidirectional manner, spacing out evenly before implantation. In the mouse, with 2D histological analysis, embryos were found in the center of the horn around 1000 h before starting a bidirectional movement on day 3 of pregnancy (Restall and Bindon, 1971). Although patterns of mouse embryo movement have been alluded to, there has been no quantitative determination of embryo spacing and the randomness of the eventual implantation sites.

Embryo movement in rabbits, rats and mice has been attributed to uterine muscle contractions. In rabbits, spontaneous uterine contractility is responsible for moving the embryo in the pre-implantation stages, by a process similar to agitation (Boving, 1956; Markee, 1944). Myogenic but not neurogenic contractions are also implicated in even embryo spacing (Kaminester and Reynolds, 1935). In rats, when relaxin, an inhibitor of alpha-adrenergic signaling, is used, embryo movement is slowed down, leading to the accumulation of embryos in the rostral segment instead of distribution along the uterine horn (Pusey et al., 1980). However, once relaxin exposure is removed, the embryos can space out evenly for implantation (Pusey et al., 1980). If relaxin is administered continuously from embryo entry until implantation, then overcrowding of embryos in the first third of the horn is observed at implantation (Rogers et al., 1983). In mice, relaxing the muscle by activating β2 adrenergic receptor (β2AR) signaling on day 3 of pregnancy disrupts embryo movement and spacing, causing crowding at implantation (Chen et al., 2011). Outcomes of mammalian pregnancy are sensitive to adrenergic signaling-regulated muscle contractions, which indicates that pregnancy responds to stress levels in the mother (Chen et al., 2013). Thus, understanding how and when adrenergic muscle contractions regulate embryo movement and spacing is crucial.

Lysophosphatidic acid (LPA) signals through G protein-coupled receptors (Sheng et al., 2015) and acts on the uterus through receptor

[1]Department of Obstetrics, Gynecology and Reproductive Biology. [2]Department of Biomedical Engineering. [3]Institute for Quantitative Health Science and Engineering, Michigan State University East Lansing, MI 48824, USA.

*Author for correspondence (ripla@msu.edu)

D.F., 0000-0003-3474-6671; M.M., 0000-0003-0001-7905; S.W., 0000-0001-6289-7448; R.A., 0000-0001-5051-6724

LPAR3. *Lpar3* is expressed in the luminal epithelium before implantation and, when deleted, affects embryo spacing and implantation (Ye et al., 2005). A link between β2AR signaling and LPAR3-signaling to mediate embryo spacing has been suggested (Chen et al., 2011). However, it is intriguing to note that causing muscle relaxation by activating the β2AR signaling causes implantation of embryo clusters at different sites along the uterine horn (Chen et al., 2011). Conversely, deleting LPAR3-mediated signaling in the uterus always causes embryo implantation in a single cluster either in the middle or closer to the cervical region of the uterus (Sheng et al., 2015; Ye et al., 2005). These observations suggest that, although both muscle contraction and LPAR3-signaling play a role in embryo spacing, they may target distinct processes in this pathway.

Understanding pre-implantation events even in a highly tractable model system such as the mouse has been challenging, in part because the peri-implantation embryo is ~100 μm in diameter, whereas the uterine horn is 2-3 cm in length and 1-1.5 mm in depth, posing a technical imaging challenge to assess both structures simultaneously. Here, using a recently developed imaging methodology for fixed uterine tissue (Arora et al., 2016), we detect embryos in the mouse after entry into the uterine horn through peri-implantation stages, documenting their location as they navigate to their implantation site. We show that embryos appear to move in two different phases, displaying either clustered or scattering movement. We further determine that, although adrenergic muscle contraction is key to the initial clustered phase, the scattering phase is independent of such muscle contractions but depends on the embryo and the LPA-LPAR3

signaling pathway. Thus, both mechanical and signaling mechanisms regulate embryo movement and spacing to achieve ideal implantation.

RESULTS
Embryo movement in the uterus occurs in phases: entry, unidirectional clustered movement and bidirectional scattering movement

We used our newly developed method (Materials and Methods, Fig. 1) to determine embryo location at the beginning of gestational day (GD) 3 at 0000 h. To assess the relative location of the embryo in the horn, we divided the uterine horn (Fig. 1A) into three equally spaced segments – segment closest to the oviduct, middle segment and a segment closest to the cervix (dashed lines in Fig. 1B) and calculated the percentage of embryos present in each section. Embryos present in the oviductal region close to the oviductal-uterine junction were accounted for in the first segment. These quantitative measurements are useful for comparing our data with the embryo location generated in the rabbit and the rat (Boving, 1956; Pusey et al., 1980; Yoshinaga et al., 1979). On GD3 at 0000 h and 0300 h, we observed embryo clusters near the oviductal-uterine junction (100% and 71% in the first uterine segment, respectively, Fig. 2, Movies 1, 2). We term this first phase in which the embryos are present in the oviduct or have just entered the uterus proximal to the oviductal-uterine junction as 'embryo entry'.

At GD3 0600 h, we observed that embryos remain in clusters but are present further along the uterine horn either in the first third (41%) or in its middle segment (53%, Fig. 2). At 0900 h and 1200 h, embryos are primarily located in clusters in the middle segment of
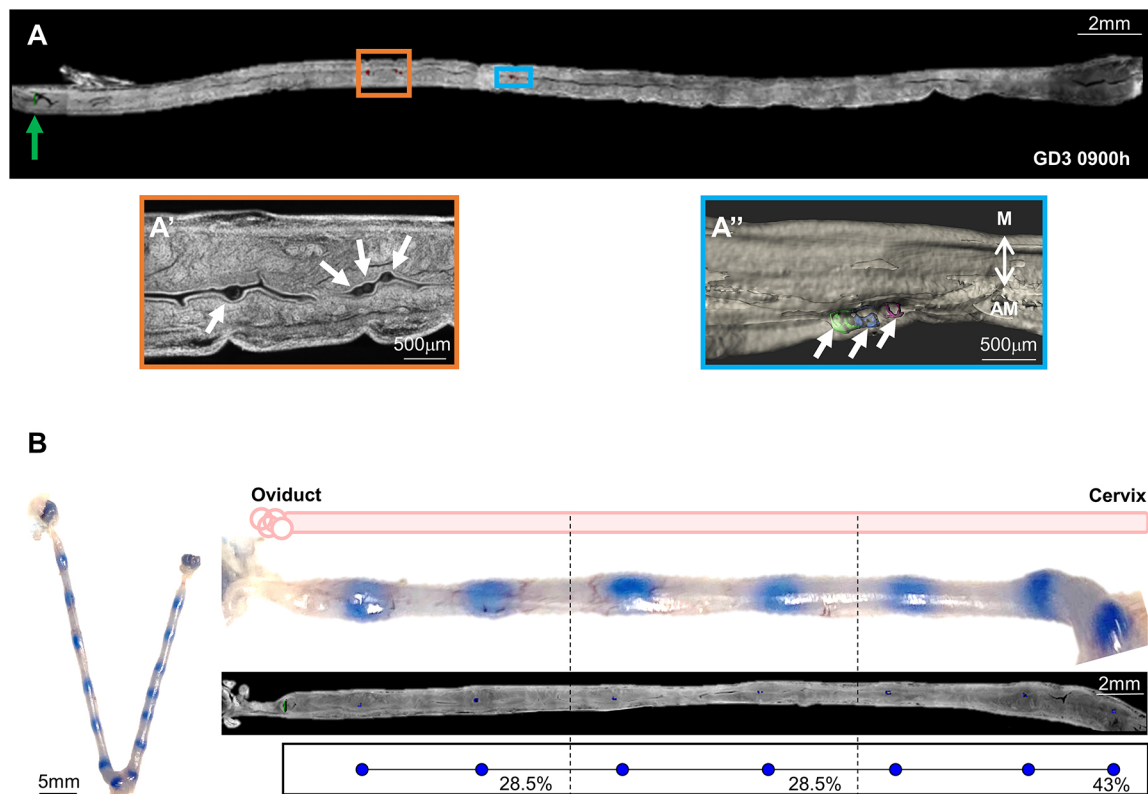

Fig. 1. Methodology to measure embryo location along the uterine horn. (A) 2D optical slice of a GD3 0900 h uterus stained with Hoechst (gray). The green arrow points to the oviductal-uterine junction. (A′) Magnified region for the orange rectangle in A showing embryos in a cluster (white arrows) on the 2D optical slice in A. (A″) Magnified region for the blue rectangle in A showing 3D reconstruction of the uterine lumen (gray) and embryo surfaces (white arrows) along the uterine horn (blue, green, pink surfaces). AM, anti-mesometrial pole; M, mesometrial pole. (B) Uterine implantation sites at GD4 1800 h shown with Evans Blue dye injections. Embryo location analysis as described in Materials and Methods. Blue circles (schematic) represent embryo location with our methodology showing similarities between the imaging-based embryo location and the blue-dye permeability method. Dashed lines divide the uterine horns into three equal segments.
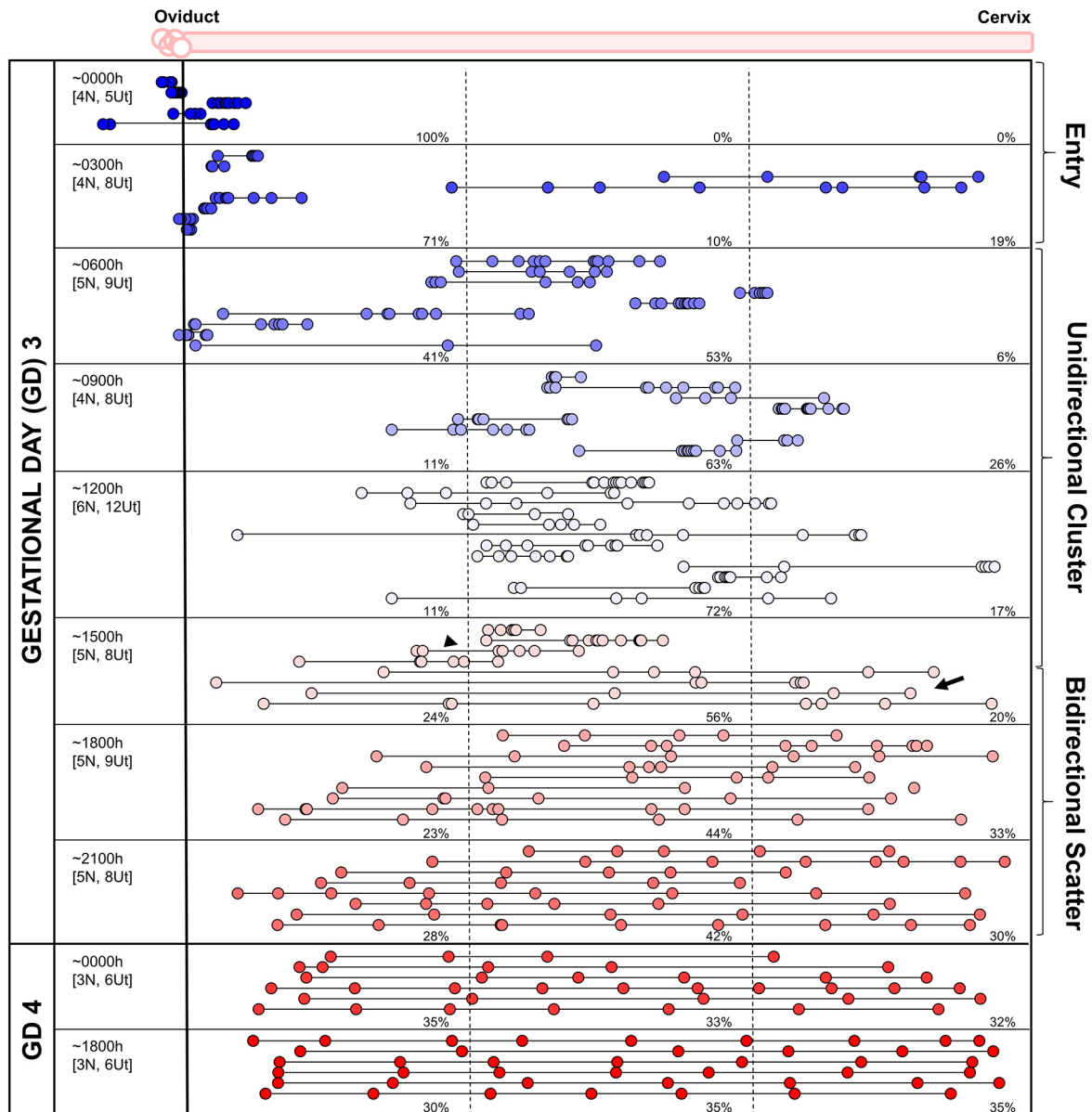
Fig. 2. Embryo movement analysis. Location of embryos in uterine horns at fixed time intervals on GD3 and GD4. Each circle represents an embryo, and circles connected with a line are embryos from the same uterine horn. Blue/white/red colors signify time scale: blue is the earliest time point on GD3, white is mid-day of GD3 and red is the latest time point on GD4. The left-hand column indicates the time of dissection in hours (h). 'N' represents the number of mice and 'Ut' represents the number of uterine horns analyzed for each time point. Dashed lines divide the uterine horns into three equal segments, and percentages for each time point signify the percentage of embryos in each segment. On GD3 at 1500 h, embryo clusters (arrowhead) and embryo scattering (arrow) can be observed.

the horn (63% and 72%, respectively, Fig. 2). Interestingly, at these time points, embryos are rarely observed near the oviductal or the cervical ends of the uterine horn (Fig. 2). When embryos are found in clusters in the first or middle segment of the uterus, they appear to have had a net unidirectional movement. We term this second phase 'unidirectional clustered movement'.

At GD3 1500 h, in half of the uterine horns, embryos are present as clusters (Fig. 2, black arrowhead). In contrast, in the other half, they are scattered and present along the entire length of the uterine horn (Fig. 2, black arrow). At 1800 h, embryos in all uterine horns are dispersed (Fig. 2) and, at 2100 h and beyond, spacing of embryos is apparent along the length of the uterine horn (Fig. 2). During this phase, embryos appear to move bidirectionally from the middle of the uterine horn to space out evenly along its entire length. We defined this third phase as 'bidirectional scattering movement'.

We compared the average number (mean±s.d.) of embryos per horn for different time points: GD3 1200 h (7.5±2.87 embryos/horn), GD4 0000 h (6.17±1.95 embryos/horn) and GD4 1800 h (7.17±0.90 embryos/horn). We did not find any significant differences between the groups (one-way ANOVA, P=0.38), suggesting no loss of embryos between embryo movement and implantation time points.

When the means of oviductal-embryo (OE) distances are plotted as a function of time, the embryos reach a value of 0.5 around GD3 0900 h (Fig. S1A). A 0.5 value signifies either the movement of embryos in a cluster and their arrival to the middle of the horn or could imply embryo spacing throughout the uterine horn. To distinguish between these two possibilities, it is essential to evaluate both OE and embryo-embryo (EE) distances as a function of time. We observe that mean values of EE distances do not start increasing until GD3 1500 h, suggesting that the clustered embryos arrive in
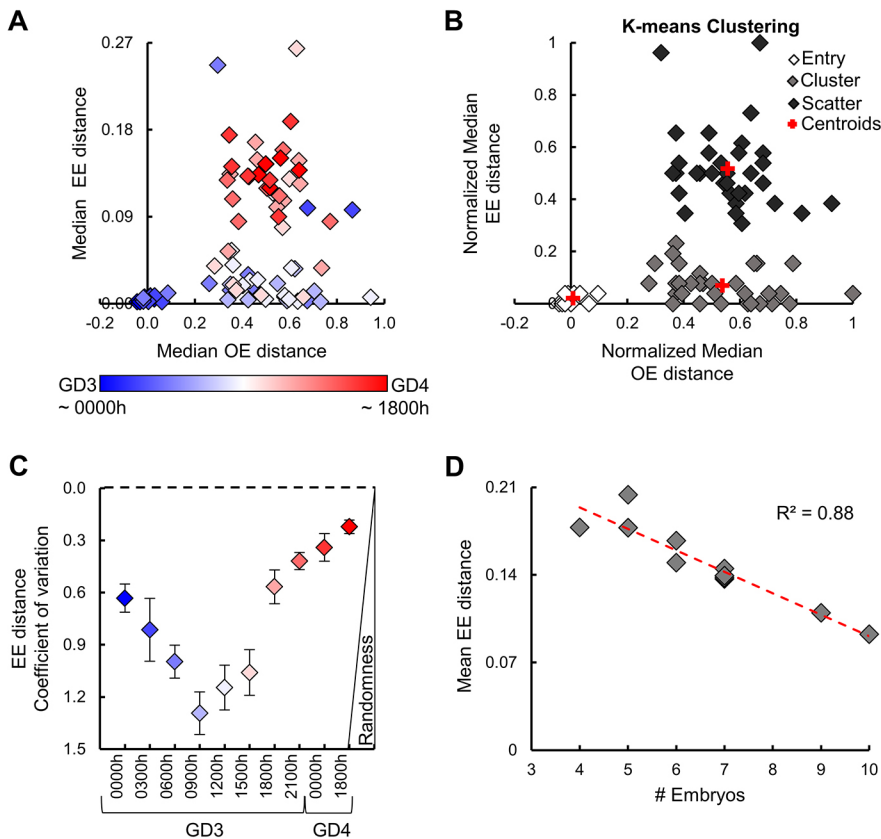
DEVELOPMENT

Fig. 3. Implantation sites are neither random nor predetermined. (A) Classification of uterine horns from Fig. 2 based on median OE and EE distance. (B) *K*-means clustering algorithm detects three clusters corresponding to the three phases: embryo entry, unidirectional embryo clusters and bidirectional embryo scattering. (C) COV of EE distances over different time points. Time points closer to implantation and post-implantation (in red) display non-random embryo spacing distribution. (D) An inverse correlation was observed between the number of embryos and EE distance for post-implantation time points (GD4 at 0000 h and 1800 h). Error bars represent s.e.m.

the middle of the horn at ∼GD3 0900 h and stay there for ∼6 h before they begin to scatter and space (Fig. S1B).

For each horn in Fig. 2, we plotted the median OE and EE distances against each other to visualize their relationship (Fig. 3A). We further performed the k-means clustering algorithm, and it automatically classified our data set into three groups (Fig. 3B) that correspond to the three embryo movement phases defined earlier (Figs 2 and 3A). When measured for OE and EE parameters, horns in each of the three phases were statistically different from each other (one-way ANOVA: OE $P<0.0001$; EE $P<0.0001$), whereas horns within the same phase were not statistically different from each other for EE parameters ($P>0.05$). This analysis also helped resolve outliers in the individual time points, for which there was a variation in embryo location likely to be a result of biological differences arising due to mating time (e.g. Fig. 2, 0300 h).

EE spacing approaches uniform distribution closer to implantation

To mathematically assess whether embryo spacing is a non-random process, we calculated the coefficient of variation (COV) of the EE distances. A larger value of COV indicates more variability in the dataset in relation to the mean of the population, i.e. a more random process. As the embryo location changes on GD3, COV varies (Fig. 3C). The value of COV goes down (GD4 0000 h, COV=0.34) at the time of attachment. This value is similar to that observed for non-random distribution of rabbit embryos (COV=0.3; Boving, 1956). Thus, even in the mouse, embryo distribution is non-random, suggesting even spacing of embryos at the time of implantation (Fig. 3C).

EE spacing is a function of embryo number

When mean EE distances were plotted as a function of the number of embryos for post-implantation time points on GD4 (0000 h and

1800 h), there was an inverse correlation between these two variables (Fig. 3D, $R^2=0.88$). We observed smaller mean EE distances in uterine horns with a larger number of embryos. To further confirm the relationship between number of embryos and EE spacing at implantation, we controlled the number of embryos in the uterine horn using surgical embryo transfer (ET). ET was performed in pseudopregnant recipient females on GD2 (1800 h), and embryo location was assessed on GD4 (1800 h) (Fig. 4) (McLaren and Michie, 1956). We noted that with ET, the first implantation site tends to be further away from the oviduct compared with natural pregnancy. Consequently, the first segment contains the lowest percentage of embryos: 13% and 23% for smaller numbers (4-6) and higher numbers (10-14) of transferred embryos, respectively (Fig. 4A). Sites of wound healing in the uterus, such as placental scars from a previous pregnancy, are refractory to embryo implantation (Momberg and Conaway, 1956). Thus, scarring from the injection site may impact embryo distribution in ET procedures.

In uteri with a low number of ET (4-6 embryos), a higher mean EE distance was observed compared with uteri with a high number of ET (10-14 embryos), in which a lower mean EE distance was observed (Fig. 4A-C). Thus, similar to natural pregnancy (Fig. 3D), in a pregnancy with ET, there is an inverse correlation between the number of embryos and the mean EE distance (Fig. 4C, $R^2=0.78$). In the ET experiments, sometimes we had only three implantation sites (Fig. 4A,C), although 4-6 embryos were transferred. This is likely owing to the efficiency of implantation post-ET. On the other hand, with our natural pregnancy analysis, the lowest number of implantation sites in a single uterine horn at GD4 was four (Fig. 3D), likely because of a larger litter size of CD1 mice (Bechard et al., 2012). To evaluate mice with only three embryos in their uterine horn through natural pregnancy, we assessed embryo location at the time of implantation in C57BL/6J females
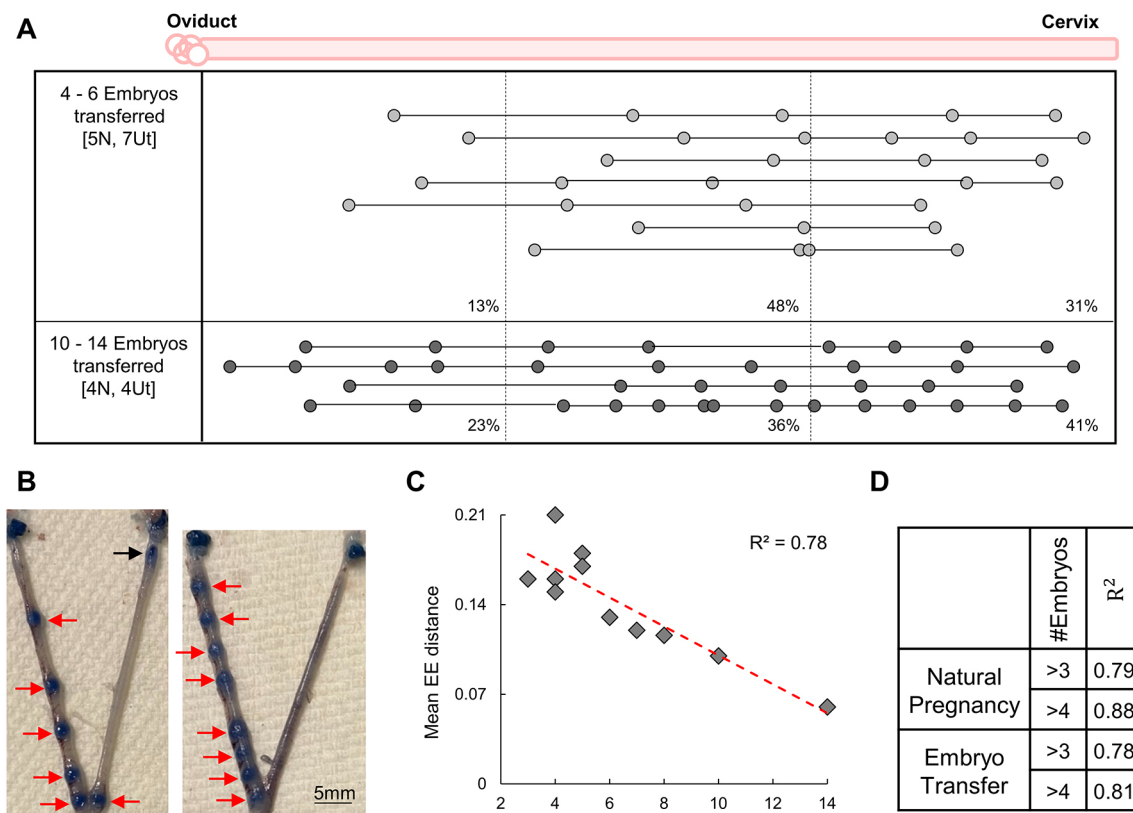
Fig. 4. Implantation sites are not predetermined, supported by controlled embryo-transfer experiments. (A) Location of transferred embryos in uterine horns on GD4 at 1800 h. Each circle represents an embryo, and circles connected with a line are embryos from the same uterine horn. The left-hand column indicates the number of transferred embryos per horn. 'N' represents the number of mice and 'Ut' represents the number of uterine horns analyzed. Dashed lines divide the uterine horns into three equal segments, and percentages for each time point signify the percentage of embryos in each segment. (B) Uterine implantation sites at GD4 1800 h of transferred embryos as seen with blue-dye injections. Red arrows, implantation site; black arrow, embryo transfer site. (C) An inverse correlation was observed between the number of embryos and EE distance for post-implantation time points (GD4 1800 h) in horns with embryo transfer. (D) The correlation coefficient for >3 or >4 embryos in natural pregnancy (from Fig. 2) and from embryo transfer.

(Fig. S2) that have a smaller litter size (Bechard et al., 2012). We combined the data for both CD1 and C57BL/6J females and observed that the correlation coefficient decreases from 0.88 when there are at least four embryos in the uterine horn to 0.79 when there are at least three embryos in the uterine horn (Fig. 4D) with natural pregnancy. This can be interpreted as a threshold of four embryos being required to achieve a strong correlation between the number of embryos and the EE distance. The COV for EE distances obtained from implantation sites at GD4 1800 h after ET was 0.35, which is similar to the COV for post-implantation time points of natural pregnancy GD4 0000 h, and 1800 h (0.34 and 0.22, respectively) and is suggestive of non-random distribution of embryos. Thus, data from both natural pregnancy and ET supports the notion that implantation sites cannot be predetermined in a non-pregnant uterus, but instead, they are guided by the number of embryos present in the uterine horn of the mouse.

Unidirectional but not bidirectional phase of embryo movement relies on adrenergic smooth muscle contractions

To test whether uterine muscle contractions regulate embryo location, we examined the effects of salbutamol, a muscle relaxant that activates β2AR signaling, by administering it at the beginning of distinct phases of embryo movement (as determined from Fig. 3B). For disrupting muscle activity in the unidirectional clustered phase (Fig. 5A), we injected salbutamol twice on GD3 at 0300 h and 1100 h and evaluated embryo location at 1500 h

(Fig. 5A). In salbutamol-injected mice, 78% of embryos were found proximal to the oviductal-uterine junction (Fig. 5A″), as opposed to vehicle-injected mice in which embryo clusters moved further along the horn and only 45% were found proximal (Fig. 5A′). These data suggest that muscle contraction during the unidirectional phase is required for clustered embryo movement through the horn. We noticed that the vehicle treatment apparently delayed the movement of embryo clusters compared with the time course data (Fig. 2). We postulate that this delay is due to the mother's stress response to the injection and endogenous activation of β-adrenergic signaling, highlighting that this phase of embryo movement is susceptible to uterine response to stress. Even still, there is a significant difference between the vehicle and the salbutamol treatment. In contrast, vehicle (Fig. 5B′) or salbutamol (Fig. 5B″) treatment at the beginning of the bidirectional phase of embryo movement (GD3 1100 h) did not alter location on GD3 at 1900 h. When median OE and EE distances were plotted, we observed that muscle relaxation inhibited clustered embryo movement resulting in both lower OE and EE values in salbutamol-treated horns compared with vehicle-treated controls (Fig. 5A‴; unpaired two-tailed t-test, OE $P<0.0002$). On the other hand, when muscle relaxation is induced before the scattering movement, the vehicle or salbutamol treatment does not affect OE and EE distance distribution (Fig. 5B‴; unpaired two-tailed t-test, OE $P=0.37$).

To determine whether the uterine muscle can recover from the effects of the muscle relaxant and how long muscle contraction is
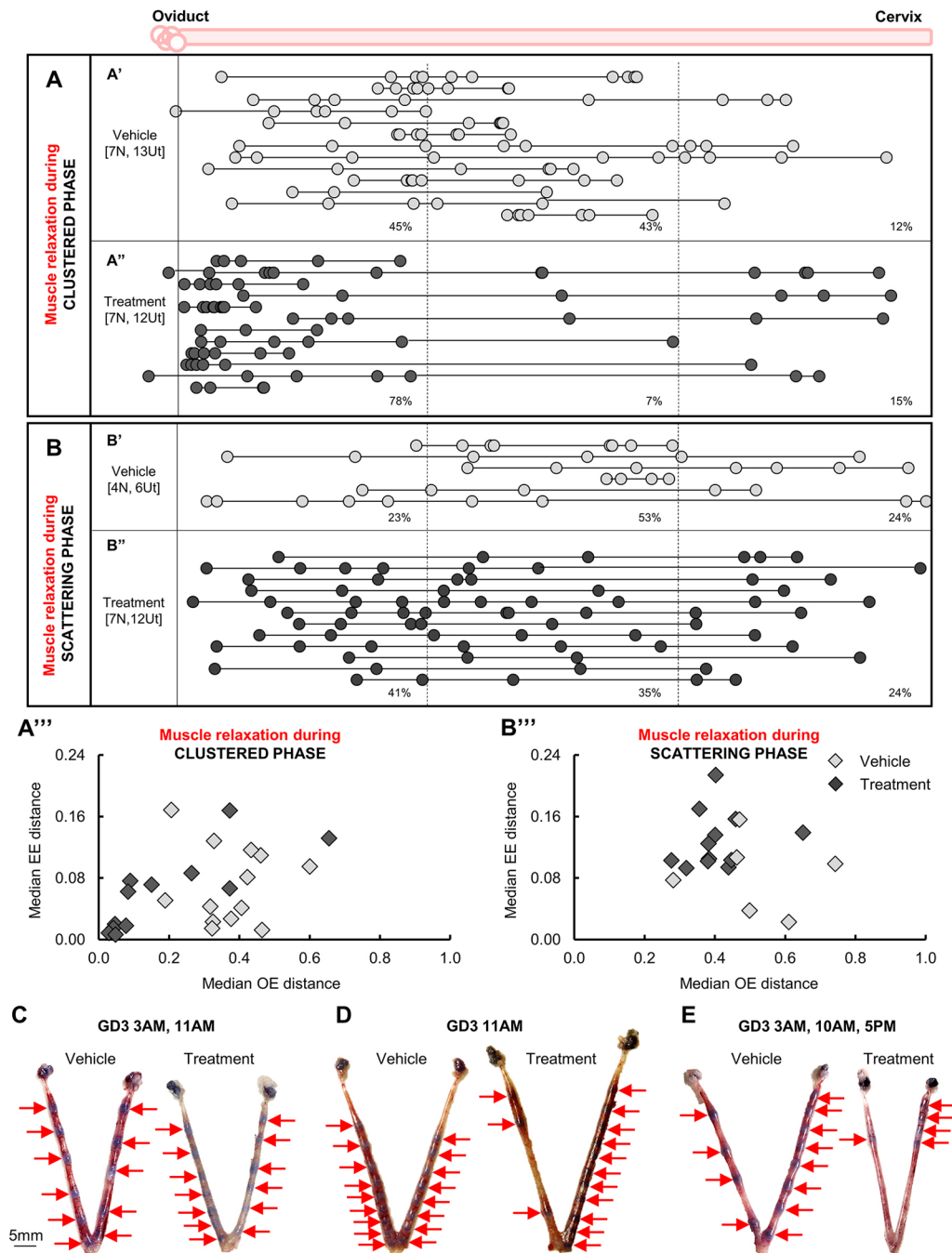
Fig. 5. Muscle contractions regulate embryo movement during the unidirectional phase but not during the bidirectional phase. (A) When the uterine muscle is treated with vehicle (A′) at the beginning of the unidirectional clustered movement phase (GD3 0300 h and 1000 h), and embryo location is assessed 12 h later (GD3 1500 h), the embryos show a distribution of 45%, 43% and 12% in the three uterine segments, respectively. On the other hand, when the uterine muscle is relaxed with salbutamol treatment (A″), 78% of the embryos are present in the first uterine segment, 7% in the second segment and 15% in the third segment, suggesting that clustered embryo movement is reliant on muscle contractions. (B) If the uterine muscle is treated with vehicle (B′) or salbutamol (B″) at the beginning of the scattering movement once embryo clusters have arrived in the middle of the uterine horn (GD3 1100 h) and embryo location is assessed 8 h later, embryo distribution is similar, suggesting that relaxing uterine muscle does not influence embryo scattering and spacing. Each circle represents an embryo, and circles connected with a line are embryos from the same uterine horn. 'N' represents the number of mice and 'Ut' represents the number of uterine horns analyzed. Dashed lines divide the uterine horns into three equal segments, and percentages for each time point signify the percentage of embryos in each segment. (A‴,B‴) Classification of uterine horns based on median OE and EE distances for embryos in A (A‴) and for embryos in B (B‴). (C-E) Analysis on GD4 1800 h to evaluate embryo location and spacing at implantation using blue-dye method when: mice are treated with vehicle or salbutamol as in A (C) or mice are treated with vehicle or salbutamol as in B (D) or when mice are treated with vehicle or salbutamol continuously (E) starting at the beginning of the unidirectional clustered phase until a few hours before attachment (GD3, 0300 h, 1000 h and 1700 h). Red arrows, implantation site.

required to allow embryo scattering and even spacing for implantation, we treated pregnant mice with salbutamol twice on GD3, at 0300 h and 1100 h as in Fig. 5A, and evaluated embryo

distribution with blue dye injection at GD4 1800 h (Fig. 5C; n=3). Embryo distribution and spacing are comparable with controls, suggesting that if the muscle has time to recover from the effects of

the muscle relaxant before implantation, embryo distribution and spacing are rescued, and embryos are spaced out evenly at implantation (Fig. 5C). On the other hand, if mice are treated with salbutamol thrice on GD3, at 0300 h, 1000 h and 1700 h, and evaluated for embryo distribution with blue dye injection at GD4 1800 h, we find that embryos are clustered during the time of implantation (Fig. 5E, *n*=4). If embryos are treated with salbutamol in the clustered phase (GD3 1100 h) and assessed for implantation at GD4 1800 h with blue dye, as expected from evaluation at GD3 1900 h (Fig. 5B), embryos are spaced evenly (Fig. 5D, *n*=3). Thus, uterine muscle contractions allow movement of the clustered embryos, provided the muscle contracts for a sufficient time before implantation.

Beads are capable of movement in the unidirectional phase but not in the bidirectional phase

Embryo movement through the uterus can be due to signaling between the embryo and the uterus, amongst the embryos, or solely caused by the physical stimulus of the embryo as an object. To distinguish between these possibilities, we injected blastocyst-sized beads in a pseudopregnant recipient uterine horn either before the unidirectional clustering phase (GD2 2200 h) or the bidirectional spacing phase (GD3 1100 h).

We injected beads near the oviductal-uterine junction before the time of embryo entry (GD2 2200 h) and evaluated 1 h later to confirm that, similar to embryos, they stay clustered upon entry and do not disperse merely due to the injection procedure. We found that beads are present as clusters, with 100% of them in the first third of the uterine horn (Fig. 6A). When they are injected near the oviductal-uterine junction before the time of embryo entry (GD2 2200 h) and evaluated 12 h later, the beads are not present in clusters. Instead, they are spread out along the uterine length, with distribution in all three segments of the uterine horn (Fig. 6B). Oviductal-bead (OB) and bead-bead (BB) distance analyses show that, at 1 h post-injection, beads are in the clustered phase, whereas at 12 h post-injection, they are already in the scattering phase (Fig. 6E). These data indicate that beads (despite being inert objects) show movement along the uterine horn when injected near the oviductal end of the uterus in the unidirectional movement phase. However, their movement pattern differs from embryos as the beads fail to move in clusters over time. Beads injected near the cervical end of the uterus and evaluated 12 h later also show unidirectional scattering movement (Fig. S3), suggesting that movement of beads is independent of the uterine end in which they are injected.

When beads were injected at the beginning of the bidirectional movement phase (GD3 1100 h) and evaluated 8 h later, they stayed in clusters and failed to display much movement or spacing away from the injection site (Fig. 6C). Bead movement was sparse irrespective of whether the beads were injected near the oviductal end (Fig. 6C) or the cervical end (Fig. 6D) of the uterus, as the majority of the beads were found in the segment where the injection site was. OB and BB analysis show that beads are stuck in clusters when injected before the beginning of the scattering phase (Fig. 6E). These results suggest that beads move in the unidirectional phase but fail to move in the bidirectional phase, highlighting that embryo-uterine or embryo-embryo interactions guide movement of embryos in the bidirectional scattering phase.

Movement in the bidirectional phase relies on embryo-uterine communication

Embryos in *Lpar3*$^{-/-}$ uteri are often found near the cervical end upon implantation, irrespective of their genotype (Ye et al., 2005).

We evaluated the location of the embryos in *Lpar3*$^{-/-}$ uteri at the end of the unidirectional clustered phase (GD3 1200 h) and during the bidirectional scattering phase (GD3 1800 h and 2100 h). Embryos in the *Lpar3*$^{-/-}$ uteri are located in clusters at GD3 1200 h, suggesting that they are capable of clustered unidirectional movement (Fig. 7A,A′; Hama et al., 2007; Ye et al., 2005). Although the embryos are present as clusters, their location displays a bias towards the third segment (closer to the cervix) in the *Lpar3*$^{-/-}$ uteri compared with the middle segment in the controls (Fig. 7A,A′, unpaired two-tailed *t*-test: OE *P*<0.0001). On the other hand, embryos in *Lpar3*$^{-/-}$ uteri are incapable of displaying bidirectional movement as they remain clustered primarily near the cervical end of the uterine horns (Fig. 7B,B′; Sheng et al., 2015). EE distances were significantly different between controls and *Lpar3*$^{-/-}$ uteri during the bidirectional scattering phase (unpaired two-tailed *t*-test: EE *P*<0.0001) but not during the unidirectional clustered phase. These data suggest that embryo-uterine communication mediated by LPAR3 fine tunes embryo cluster movement in the unidirectional phase but plays a crucial role in embryo movement during the bidirectional phase.

DISCUSSION

Using 3D imaging to capture the entire uterine structure, along with embryos and their location, we provide a detailed quantitative analysis of early events in mammalian pregnancy. Previous work in the mouse on embryo spacing has been performed in either whole mount at a time when the implantation sites or embryonic deciduae occupy a substantial portion of the uterine horn (Hollander and Strong, 1950) or as 2D histological sections near the time of implantation (Restall and Bindon, 1971). To make accurate estimates of even and uneven spacing, embryo distribution analysis needs to be performed when the object to be distributed (the embryo) occupies less than 5% of the area it will be distributed in (the uterine horn) (Boving, 1956). Although the vascular permeability reaction (Psychoyos, 1961) has been used to mark mouse implantation sites, it is first observed only on GD3 at 1800 h, and only 10% of the embryos are detected. It is not until GD4 at 1500 h that 100% of the embryos display a positive blue dye reaction (Restall and Bindon, 1971). Our methodology offers advantages over the blue-dye method as it can estimate embryo location accurately at pre-implantation time points, at which, owing to the lack of increase in vascular permeability, the blue-dye method fails. Further, because we label and scan the whole uterine tissue, there is no loss of information due to technical challenges and human error, as in the case of 2D histological sections. Thus, we applied our methodology to carry out quantitative embryo location analysis in the mouse during peri-implantation events.

Embryo location and movement: similarities and differences between mammalian species

Previous work with model organisms of mammalian pregnancy, such as the rat and the rabbit, has provided detailed quantitative descriptions of events of early embryo movement through the uterine tissue. Using a mouse model, we find differences and similarities compared with previous results in rat and rabbit models.

Embryo entry

Although it has been mentioned that embryo entry into the uterus occurs early on GD3 (Hama et al., 2007; Potts and Wilson, 1967), no morphological data has been presented. We observed embryo clusters near the oviductal-uterine junction at the beginning of GD3. Embryos may have entered the uterus one by one, but they did not move far
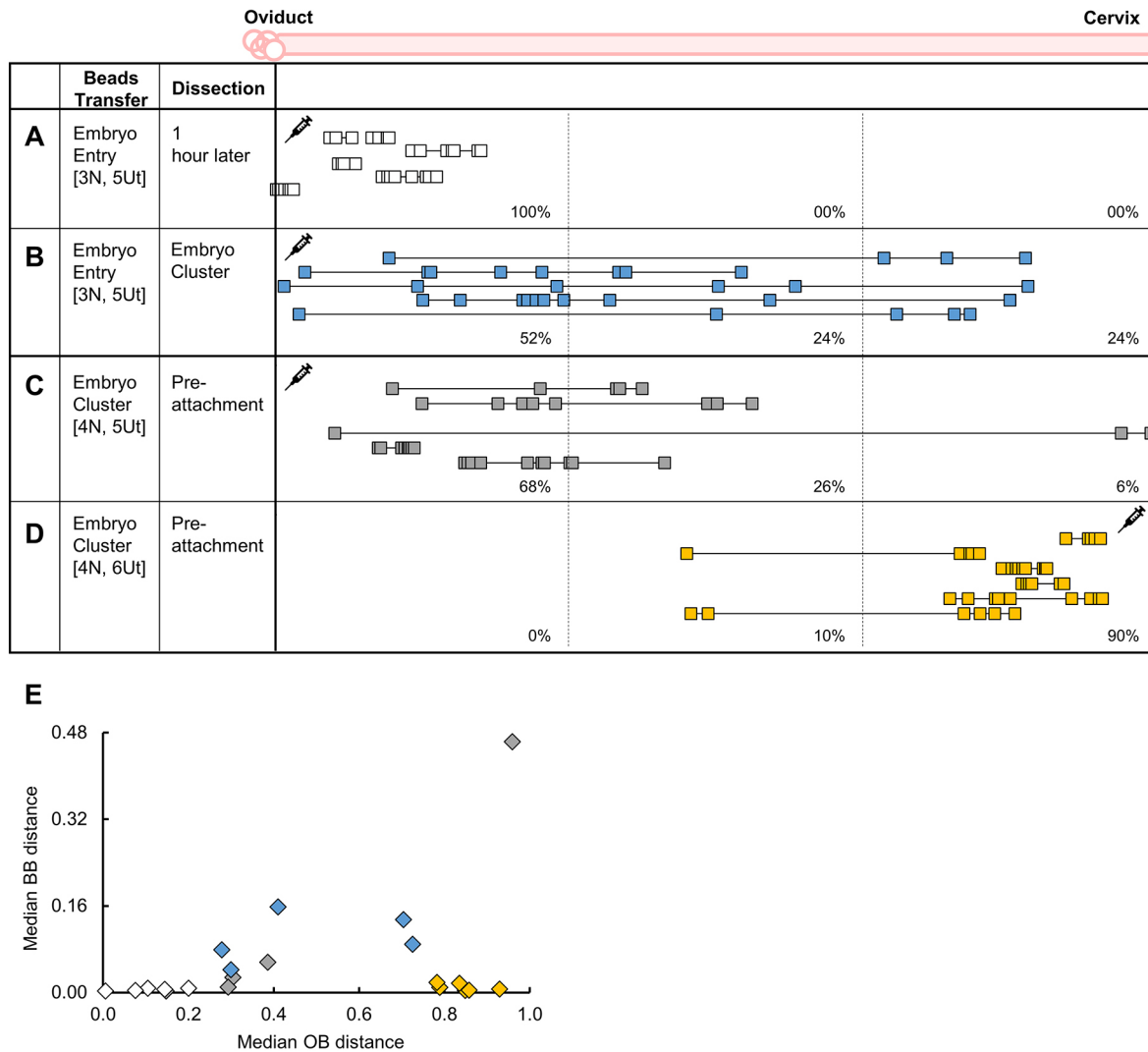
7

Fig. 6. Inert beads move during the unidirectional phase but not during the bidirectional phase. (A-D) Beads injected near the oviductal-uterine junction at the time of embryo entry appear to move in clusters 1 h post-injection (A) but are scattered along the uterine horn 12 h post-injection (B). Beads injected at the beginning of the scattering phase near the oviductal-uterine junction (C) or near the cervical region of the uterus (D) stay primarily near the site of injection and do not move much. Each square represents a bead, and beads connected with a line are beads from the same uterine horn. 'N' represents the number of mice and 'Ut' represents the number of uterine horns analyzed. Dashed lines divide the uterine horns into three equal segments, and percentages for each time point signify the percentage of beads in each segment. (E) Median OB and BB distance of uterine horns in A, B, C and D. Syringe needle indicates location of bead injection site (near the oviductal-uterine junction or near the cervical region of the uterus).

away from the oviductal-uterine junction until all the embryos had entered the uterus. It is also possible that, similar to the rabbit (Boving, 1956), mouse embryos enter together as small clusters and not one by one, but the only way to distinguish between these possibilities is using live imaging, which as yet has not been possible.

Movement through the horn
Our static location data suggests that, in the mouse, embryos move in clusters during the first phase of movement. In rats, irrespective of the time point analyzed, embryos are always found in the first segment of the uterine horn (Pusey et al., 1980), and in the rabbit, blastocyst progression is continuous, based on the mean/median embryo location and the progressive increase in the EE distance (Boving, 1956). This suggests that embryos in the rat and the rabbit uterus enter, scatter and space out unidirectionally (Fig. 8). These data are in contrast to our results in the mouse, as there are time points at which embryos are sparsely found in the first third of the

uterine horn, and EE distances stay small in the unidirectional phase and only start to increase in the bidirectional scattering phase (Fig. 8). It is important to note that, while embryos are moving through the uterine horn, the uterine lumen undergoes closure at about 85 h post-coitus (Wilson, 1962), which would be comparable with our GD3 1500 h time point. This is precisely when half of our mice displayed clustered embryos, and the other half started to scatter. We speculate that luminal closure may guide the switch between clustered and scattered localization of embryos. Further studies are needed to assess the impact of embryo size and luminal diameter to regulate unidirectional versus bidirectional patterns of embryo movement. It has been hypothesized that luminal closure occurs due to fluid resorption and plays a major role in locking the embryo in place (Chen et al., 2013; Davidson and Coward, 2016). Thus, factors that regulate fluid resorption including hormones (progesterone; Clemetson et al., 1977; Salleh et al., 2005), genetic factors (FOXO1; Vasquez et al., 2018) and ion channels (Na+;
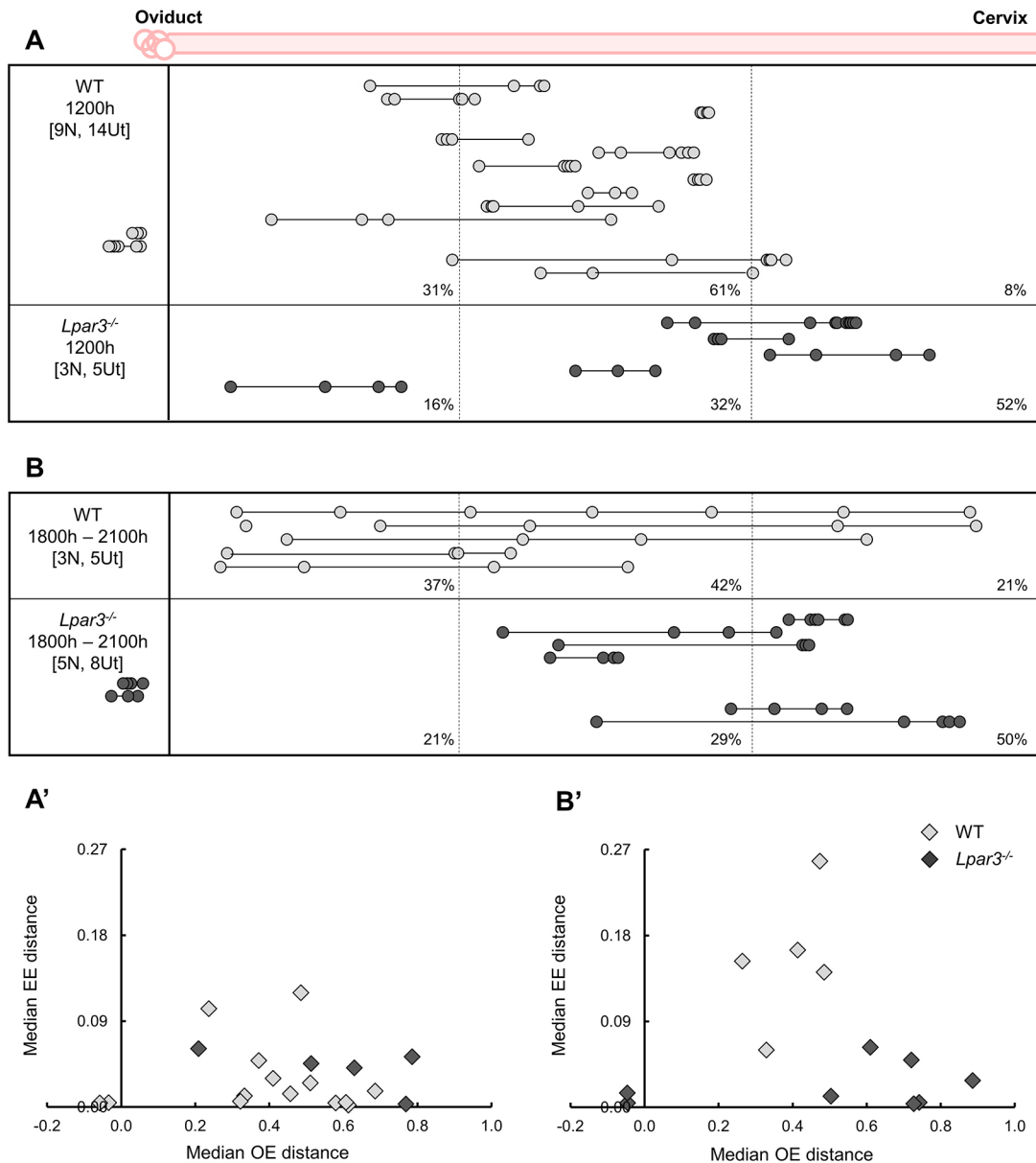
8

Fig. 7. LPAR3-dependent embryo-uterine communication is essential for the bidirectional scattering of embryos. (A) Embryos are present in clusters in the middle and cervical segments of the control and *Lpar3*^{−/−} uteri at the end of the unidirectional clustered movement phase (GD3 1200 h). (A′) Median OE and EE distance of uterine horns in A. (B) Whereas embryos in the control horns scatter between GD3 1800 h and 2100 h, embryos in *Lpar3*^{−/−} horns are stuck near the cervix in clusters. (B′) Median OE and EE distance of uterine horns in B. Each circle represents an embryo, and circles connected with a line are embryos from the same uterine horn. 'N' represents the number of mice and 'Ut' represents the number of uterine horns analyzed. Dashed lines divide the uterine horns into three equal segments, and percentages for each time point signify the percentage of embryos in each segment.

Nobuzane et al., 2008) might be involved in the switch between the two phases of movement.

There appears to be an absence of clustered movement in the rabbit, but there is always a separation between blastocyst location and the end zones of the uterus, implying blastocysts are not present near the oviductal or cervical ends of the uterus (Boving, 1956). This is similar to the end of the clustered phase movement in the mouse, in which embryos are close to each other but far off from either end of the uterus. Evolutionarily, why there is a time when both ends of the uterus in the mouse and the rabbit do not contain embryos is an intriguing observation and warrants further investigation. In contrast to previous data with the mouse (Restall and Bindon, 1971), where embryo spacing is suggested to begin at 1000 h, our data clearly

shows that embryos stay clustered and start spacing around 1500 h on GD3.

Spacing and implantation
Although there are differences in how embryos move through the uterine horn and the sequence in which they achieve spacing, rats (O'Grady and Heald, 1969; Pusey et al., 1980), rabbits (Boving, 1956) and mice (this study) all show even embryo spacing at the time of implantation as determined by the COV of the EE distances. This, along with the fact that uterine horns vary in length, and EE distance post-implantation is inversely proportional to the number of embryos in the uterine horn, either during natural pregnancy or with ET, supports the idea that implantation sites are not
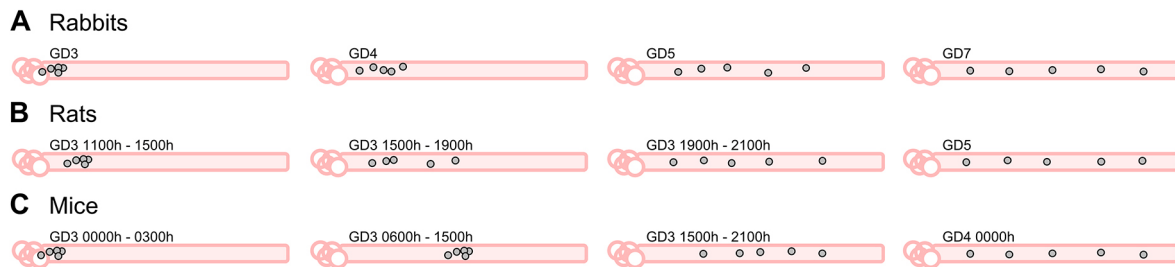
Fig. 8. Schematic of embryo movement in three models. (A-C) Schematic of embryo movement for rabbits (A), rats (B) and mice (C). Although rabbits and rats display unidirectional clustered and scattered movements to achieve embryo spacing, mice employ a unidirectional clustered movement phase followed by a bidirectional scattering and spacing phase of embryo movement.

predetermined but are formed once embryos enter the horn and begin interacting with the uterine environment.

Adrenergic muscle contraction is responsible for embryo movement but not embryo spacing

We determined that adrenergic uterine contractions are required for the unidirectional movement of embryo clusters but not the bidirectional movement for embryo scattering. Although interfering with contractile activity before embryo arrival at the center of the horn causes overcrowding of embryos and compromises pregnancy outcomes (Chen et al., 2011; this study), it is key to note that, similar to in rat studies (Pusey et al., 1980; Rogers et al., 1983), overcrowding of embryos at implantation depends on the amount of recovery time between removal of the muscle relaxant stimulus and embryo attachment. A 7-h gap between the last injection of salbutamol and embryo implantation does not allow sufficient movement, and embryos overcrowd at attachment. On the other hand, a 13-h recovery period between the last injection of salbutamol and embryo attachment allows for embryo movement, presumably once the effect of the muscle relaxant wears off, and spacing is observed at GD4. Because spacing is achieved in a shortened window of time, either (1) the embryos increase their speed of movement to achieve even spacing before attachment, (2) embryos alter their movement by picking a different unidirectional or bidirectional pattern, or (3) embryos start out by displaying unidirectional movement as the uterus recovers from the last salbutamol treatment, but then switch from unidirectional to bidirectional movement mid-way. We speculate that once the embryos are positioned in the center of the horn and the uterus has presumably counted the embryos, the adrenergic uterine contractions do not play a role in embryo spacing in the mouse.

Inert objects display movement in the unidirectional clustered phase but fail to do so in the bidirectional scattering phase

Beads as inert objects appear to move in the uterine horn only in the first phase of movement and not during the second phase. Further, although bead movement begins as clusters, the beads eventually disperse and break out of clusters, suggesting that movement in clusters could require embryo-embryo or embryo-uterine interactions. Bead movement in the unidirectional phase, along with our data that muscle contraction is required for embryo movement during the unidirectional phase, suggests that object movement is passive and under the regulation of uterine peristalsis in this phase. This passive movement is time-sensitive, as uterine contractile activity by itself was not enough to move beads during the scattering phase. Thus, the second phase of movement relies on active communication between the embryo and the uterus to facilitate even spacing throughout the horn.

LPA-LPAR3 signaling plays a role in the bidirectional scattering phase of embryo movement

An embryo is key to even spacing, but studies with genetic mutants in which control embryos are incapable of spacing in gene-deleted uteri [e.g. *Lpar3* (Ye et al., 2005) and *cPla2* (Song et al., 2002)] suggest that there is an active embryo-uterine component to embryo spacing. Because *Lpar3* mRNA was downregulated in the salbutamol-treated uteri (Chen et al., 2011), but patterns of overcrowding are distinct between *Lpar3*$^{-/-}$ mice (embryo crowding in a single cluster, near the cervix) and salbutamol-treated mice (embryo crowding in multiple clusters at different sites along the uterine horn), we wanted to determine the effects of *Lpar3* deletion on embryo distribution and location. Our study indicates that in *Lpar3*$^{-/-}$ uteri, embryos travel through the uterine horn unidirectionally as clusters, but the precise location of these clusters is regulated by the LPA-LPAR3 signaling pathway. This is not surprising, as LPAR3-mediated signaling has been implicated in uterine contractions (Hama et al., 2007). Although *Lpar3*$^{-/-}$ uteri display movement in the unidirectional phase, they do not respond to the embryos to initiate the bidirectional scattering movement. Thus, embryo-uterine communication mediated by LPAR3 is crucial to embryo movement and spacing during the bidirectional movement phase.

Boving has implied that muscle activity that propels embryo movement is distinguished by either spontaneous contractions or stimulated contractions (Boving, 1956). Spontaneous contractions can be induced by prostaglandins (such as PGF2α) and are suppressed by estrogen and relaxin (Porter et al., 1979). On the other hand, progesterone acts on uterine muscle by conditioning it and reducing the spread of contractile activity (Csapo, 1955). Stimulated contractions are likely induced by the embryo itself. We speculate that the first phase of the unidirectional clustered movement is under the influence of spontaneous contractions that involve the adrenergic signaling pathway. These contractions are likely inhibited at the time of the nidatory peak of estrogen (McCormack and Greenwald, 1974), and movement of embryos is then guided by embryo-stimulated contractility of the uterus. These second set of contractions are likely under the regulation of ovarian hormone progesterone and LPAR3, and these stimulated contractions ensure equal spacing of embryos before implantation.

Physical embryo movement is significant not only for small mammals but also for larger animals such as cats, dogs, pigs and horses. Embryo mobility in the cat (Tsutsui et al., 1989), dog (Tsutsui et al., 2002) and pig (Sittmann, 1973) is essential for transuterine migration. This is because, unlike in the mouse, embryos in these species can move across the uterine horns to equalize the number of embryos in each horn. In the pig and horse, it has been conclusively shown that embryo movement is also

essential for pregnancy success. When embryo mobility is restricted in the pig, either by limiting embryos to one horn or by ligating the uterine horn, the entire pregnancy was lost (Dhindsa and Dziuk, 1968; Dziuk, 1985). Similarly, embryos in mares must be able to travel across at least two-thirds of the endometrial surface, as uterine ligatures that reduce this surface cause pregnancy failure (McDowell et al., 1988). Interestingly uterine ligation in the mare reduces the levels of serum progesterone, suggesting a direct link between mechanical stimulus of the embryo and induction of ovarian progesterone essential for signaling. Similar to rodents and rabbits, uterine contractions have also been implicated in embryo mobility in the pig (Dhindsa et al., 1967) and the horse (Ginther, 1985; Leith and Ginther, 1985). In humans, embryo movement under the influence of uterine contractions and intraluminal uterine fluid flow has shown to be important for embryo survival. Women with hydrosalpinx have an increase in tubal pressure creating a pressure gradient between the fundus and the cervix. This pressure gradient adversely affects the cervix-to-fundus myometrial contractions and is predicted to thrust the embryo away from a viable area for implantation. Thus, even in humans, embryo mobility is essential to navigate the site of implantation, and uterine contractions regulate this movement of the embryo (Eytan et al., 2001). Exploring the mechanisms of embryo movement in the mouse model opens up avenues to understanding these events in larger animals and primates.

Our study provides a deeper understanding of the mouse embryo movement process that could depend on physical forces (muscle contractions) or signaling mechanisms (mediated by the embryo or/ and the LPA-LPAR3 pathway). This understanding is essential because modulating these processes will be key to manipulating early events in implantation for pregnancy success and developing novel methods of contraception.

MATERIALS AND METHODS
Animals
All animal research was carried out under the guidelines of the Michigan State University Institutional Animal Care and Use Committee. CD1 (ICR), wild-type C57BL/6J, and $Lpar3^{tm1JCh}$ ($Lpar3^{-/-}$) mice (Ye et al., 2005), aged 6 to 8 weeks, were maintained on a 12 h light/dark cycle. Adult females were mated with fertile or vasectomized wild-type males to induce pregnancy or pseudopregnancy. The appearance of a vaginal plug was identified as GD0.5. For CD1 females, uterine dissections were performed at 3-h intervals, starting from midnight on GD3 at 0000 h until GD4 at 0000 h and on GD4 at 1800 h, whereas in $Lpar3^{-/-}$ (C57BL/6J background) and C57BL/6J, they were performed at 1200 h or between 1800 h and 2100 h on GD3. A minimum of three mice were analyzed for each condition to ensure data reproducibility in independent events. For detecting implantation sites on GD4 at 1800 h, 200 μl of 0.5% Evans Blue dye (MP Biomedicals, ICN15110805) in phosphate-buffered saline (PBS) was injected into the lateral tail vein of the pregnant mouse 15 min before sacrificing the mouse. Uteri were then photographed in white light to observe implantation sites (Psychoyos, 1961).

Embryo harvest
Embryos were collected from pregnant females on GD3 between 1200 h and 1500 h by flushing the uterine horn using M2 medium (Sigma-Aldrich, M7167). The embryos were washed three times in M2 medium then moved to M2 medium drops under mineral oil (Sigma-Aldrich, M8410) in 5% CO_2 and a 37°C incubator until the embryo transfer surgery (Li et al., 2015).

Embryo transfer
A Pasteur pipette (Fisher, 13-678-20C) was pulled on a flame smoothly to produce a pipette tip of an internal diameter ranging between 150 and 300 μm. To obtain an even tip, the pipette tip was fire polished by quickly touching the flame. Using mouth pipetting, the tip was loaded with either 4-6 embryos or 10-14 embryos along with two air bubbles. The air bubbles aid in visualizing successful embryo transfer. The uterine wall was punctured with a 27-gauge needle near the oviductal-uterine junction region. The pipette tip was introduced through this puncture, and the embryos were blown slowly into the lumen. Embryo transfer surgeries were performed between 1800 h and 2100 h on GD2 of pseudopregnancy. Mice were sacrificed on GD4 at 1800 h, and implantation sites were detected using Evans Blue dye as described above.

Beads transfer
For surgical bead transfer Pasteur pipettes similar to embryo transfer were used. Using mouth pipetting, the tip was loaded with spherical agarose beads in PBS (4-10 beads/horn; Affi-Gel Blue Media, 153-7302) with 75-150 μm in diameter along with two air bubbles. The air bubbles aid in visualizing successful bead transfer. The uterine wall was punctured with a 27-gauge needle either near the oviductal-uterine junction or the uterine region closest to the cervix. The pipette tip was introduced through this puncture, and the beads were blown slowly into the lumen. Bead transfer surgeries were performed between 2000 h and 2400 h on GD2 of pseudopregnancy, or at 1100 h on GD3 of pseudopregnancy. Mice were sacrificed on GD3 at 1200 h or 2100 h.

Drug treatments
Salbutamol (Alfa Aesar, A18544) was dissolved in a 10% ethanol solution made in PBS and injected intraperitoneally at 2 mg/mouse (Chen et al., 2011). Mice in the vehicle group received injections of a 10% ethanol in PBS solution. Vehicle or salbutamol was administered on GD3 either once at 1100 h, twice at 0300 h and 1100 h, or thrice at GD3 0300 h, 1000 h and 1700 h.

Whole-mount immunofluorescence
Whole-mount immunofluorescence was performed as described previously (Arora et al., 2016). Briefly, uteri were dissected and fixed in DMSO:methanol (1:4), rehydrated for 15 min in 1:1 methanol:PBST (PBS, 1% Triton X-100) solution, followed by a 15 min wash in 100% PBST solution. Samples were incubated in a blocking solution (PBS, 1% Triton X-100, 2% powdered milk) for 2 h at room temperature. Uteri were incubated with primary antibodies diluted in blocking solution (1:500) for five nights at 4°C. Subsequently, the samples were washed six times for 30 min each using PBST and then incubated with secondary antibodies diluted in PBST (1:500) for two nights at 4°C. The uteri were then washed six times for 30 min each using PBST, followed by a 30 min dehydration in 100% methanol, an overnight incubation in 3% H_2O_2 solution diluted in methanol, and a final dehydration step for 30 min in 100% methanol. Samples were cleared using a 1:2 mixture of benzyl alcohol:benzyl benzoate (Sigma-Aldrich, 108006, B6630).

The primary antibody used was ECAD (M106, Takara Biosciences) (Arora et al., 2016). The secondary antibodies, conjugated Alexa Flour IgGs, were obtained from Invitrogen (A31572 and A21247), and Hoechst (Sigma Aldrich, B2261) was used to stain the nucleus.

Confocal microscopy
Uteri were imaged using a Leica TCS SP8 X Confocal Laser Scanning Microscope System with white-light laser, using a 10x air objective. For each uterine horn, z-stacks were generated with a 7.0 μm increment, and tiled scans were set up to image the entire length and depth of the uterine horn (Arora et al., 2016). Images were merged using Leica software LASX version 3.5.5 (Fig. 1A).

Image analysis for embryo location
Commercial software Imaris v9.2.1 (Bitplane) was used for image analysis. The confocal LIF files were imported into the Surpass mode of Imaris. For embryo location analysis, structures of the oviductal-uterine junction (green arrow), embryos (white arrows), beads and horns were created as 3D renderings using the Surface module (Fig. 1A-A″). With the Measurements module, the three-dimensional Cartesian coordinates of the center of each surface were identified and stored. The Cartesian coordinates of the orthogonal projection onto the x-y plane were used to calculate the distance between the oviductal-uterine junction and an embryo (OE), the oviductal-

uterine junction and a bead (OB), adjacent embryos (EE), adjacent beads (BB) and the horn length. All distances were normalized to the horn length to compensate for uterine horn length differences amongst mice. Thus, the mean values for OE, EE, OB and BB distances are a ratio and unitless. In order to obtain a meaningful mean EE distance per uterine horn, a minimum of three embryos is required. Therefore, horns with less than three embryos/beads were excluded from the analysis. Finally, these distances were used to map the embryo/bead location relative to the length of the uterine horn. To confirm the robustness of our embryo location method, we compared the results of our embryo location analysis to the established blue-dye injection method at the time of embryo implantation (Psychoyos, 1961). When we compare our embryo location data at GD4 1800 h, it overlaps with the data generated using a blue-dye permeability assessment (Fig. 1B).

Coefficient of variation
We computed the COV as the standard deviation of EE distances divided by the mean of the EE distances for each horn of the time points assessed (Boving, 1956). The mean value of all COVs for all horns at a particular time point was plotted as a function of time.

k-means clustering
The relationship between OE and EE median distances was analyzed using the *k*-means clustering algorithm implemented on MATLAB. This method aims to divide *n* data points into *k* clusters in which each data point belongs to the cluster with the nearest mean (cluster centroid). As a preprocessing step for *k*-means analysis, each dataset was normalized to a range −1 to 1 (Jain et al., 1999).

Statistical analysis
Statistical analyses were performed using Graph Pad Prism. One-way analysis of variance (ANOVA) ANOVA was used to statistically analyze OE and EE distances amongst uterine horns and different time points. To compare the vehicle and the treatment for muscle contraction analysis, and the $Lpar3^{-/-}$ with controls, the unpaired two-tailed *t*-test was performed with Welch's correction.

Supplementary information
Supplementary information available online at
https://dev.biologists.org/lookup/doi/10.1242/dev.193490.supplemental

Peer review history
The peer review history is available online at
https://dev.biologists.org/lookup/doi/10.1242/dev.193490.reviewer-comments.pdf

References
Arora, R., Fries, A., Oelerich, K., Marchuk, K., Sabeur, K., Giudice, L. C. and Laird, D. J. (2016). Insights from imaging the implanting embryo and the uterine environment in three dimensions. *Development* **143**, 4749-4754. doi:10.1242/dev.144386

Bechard, A., Nicholson, A. and Mason, G. (2012). Litter size predicts adult stereotypic behavior in female laboratory mice. *J. Am. Assoc. Lab. Anim. Sci.* **51**, 407-411.

Böving, B. G. (1956). Rabbit blastocyst distribution. *Am. J. Anat.* **98**, 403-434. doi:10.1002/aja.1000980305

Bulletti, C. and de Ziegler, D. (2005). Uterine contractility and embryo implantation. *Curr. Opin. Obstet. Gynecol.* **17**, 265-276. doi:10.1097/01.gco.0000169104.85128.0e

Chen, Q., Zhang, Y., Peng, H., Lei, L., Kuang, H., Zhang, L., Ning, L., Cao, Y. and Duan, E. (2011). Transient β_2-adrenoceptor activation confers pregnancy loss by disrupting embryo spacing at implantation. *J. Biol. Chem.* **286**, 4349-4356. doi:10.1074/jbc.M110.197202

Chen, Q., Zhang, Y., Elad, D., Jaffa, A. J., Cao, Y., Ye, X. and Duan, E. (2013). Navigating the site for embryo implantation: biomechanical and molecular regulation of intrauterine embryo distribution. *Mol. Asp. Med.* **34**, 1024-1042. doi:10.1016/j.mam.2012.07.017

Clemetson, C. A. B., Verma, U. L. and De Carlo, S. J. (1977). Secretion and reabsorption of uterine luminal fluid in rats. *J. Reprod. Fertil.* **49**, 183-187. doi:10.1530/jrf.0.0490183

Csapo, A. (1955). The mechanism of myometrial function and its disorders. In *Modern Trends in Obstetrics and Gynaecology* (ed. K. Bowes), pp. 20-49. London: Butter-worth and Co., Ltd.

Davidson, L. M. and Coward, K. (2016). Molecular mechanisms of membrane interaction at implantation. *Birth Defects Res. C Embryo Today* **108**, 19-32. doi:10.1002/bdrc.21122

Dhindsa, D. S. and Dziuk, P. J. (1968). Influence of varying the proportion of uterus occupied by embryos on maintenance of pregnancy in the pig. *J. Anim. Sci.* **27**, 668-672. doi:10.2527/jas1968.273668x

Dhindsa, D. S., Dziuk, P. J. and Norton, H. W. (1967). Time of transuterine migration and distribution of embryos in the pig. *Anat. Rec.* **159**, 325-330. doi:10.1002/ar.1091590309

Dziuk, P. (1985). Effect of migration, distribution and spacing of pig embryos on pregnancy and fetal survival. *J. Reprod. Fertil. Suppl.* **33**, 57-63.

Eytan, O., Azem, F., Gull, I., Wolman, I., Elad, D. and Jaffa, A. J. (2001). The mechanism of hydrosalpinx in embryo implantation. *Hum. Reprod.* **16**, 2662-2667. doi:10.1093/humrep/16.12.2662

Ginther, O. J. (1985). Dynamic physical interactions between the equine embryo and uterus. *Equine Vet. J.* **17**, 41-47. doi:10.1111/j.2042-3306.1985.tb04592.x

Hama, K., Aoki, J., Inoue, A., Endo, T., Amano, T., Motoki, R., Kanai, M., Ye, X., Chun, J., Matsuki, N. et al. (2007). Embryo spacing and implantation timing are differentially regulated by LPA3-mediated lysophosphatidic acid signaling in mice. *Biol. Reprod.* **77**, 954-959. doi:10.1095/biolreprod.107.060293

Hollander, W. F. and Strong, L. C. (1950). Intra-uterine mortality and placental fusions in the mouse. *J. Exp. Zool.* **115**, 131-149. doi:10.1002/jez.1401150108

Jain, A. K., Murty, M. N. and Flynn, P. J. (1999). Data clustering: a review. *ACM Comput. Surv.* **31**, 264-323. doi:10.1145/331499.331504

Kaminester, S. and Reynolds, S. R. M. (1935). Motility in the transplanted, denervated uterus. *Am. J. Obstet. and Gynec.* **30**, 395-402. doi:10.1016/S0002-9378(16)41187-7

Leith, G. S. and Ginther, O. J. (1985). Mobility of the conceptus and uterine contractions in the mare. *Theriogenology* **24**, 701-711. doi:10.1016/0093-691X(85)90169-4

Li, S.-J., Wang, T.-S., Qin, F.-N., Huang, Z., Liang, X.-H., Gao, F., Song, Z. and Yang, Z.-M. (2015). Differential regulation of receptivity in two uterine horns of a recipient mouse following asynchronous embryo transfer. *Sci. Rep.* **5**, 15897. doi:10.1038/srep15897

Markee, J. E. (1944). Intrauterine distribution of ova in the rabbit. *Anat. Rec.* **88**, 329-336. doi:10.1002/ar.1090880402

McCormack, J. T. and Greenwald, G. S. (1974). Evidence for a preimplantation rise in oestradiol-17beta levels on day 4 of pregnancy in the mouse. *J. Reprod. Fertil.* **41**, 297-301. doi:10.1530/jrf.0.0410297

McDowell, K. J., Sharp, D. C., Grubaugh, W., Thatcher, W. W. and Wilcox, C. J. (1988). Restricted conceptus mobility results in failure of pregnancy maintenance in mares. *Biol. Reprod.* **39**, 340-348. doi:10.1095/biolreprod39.2.340

McLaren, A. and Michie, D. (1956). Studies on the transfer of fertilized mouse eggs to uterine foster-mothers. I. Factors affecting the implantation and survival of native and transferred eggs. *J. Exp. Biol.* **33**, 394-416.

Momberg, H. and Conaway, C. (1956). The distribution of placental scars of first and second pregnancies in the rat. *J. Embryol. Exp. Morphol.* **4**, 376-384.

Nobuzane, T., Tashiro, S. and Kudo, Y. (2008). Morphologic effects of epithelial ion channels on the mouse uterus: differences between raloxifene analog (LY117018) and estradiol treatments. *Am. J. Obstet. Gynecol.* **199**, 363.e1-363.e6. doi:10.1016/j.ajog.2008.03.047

O'Grady, J. E. and Heald, P. J. (1969). The position and spacing of implantation sites in the uterus of the rat during early pregnancy. *J. Reprod. Fertil.* **20**, 407-412. doi:10.1530/jrf.0.0200407

Porter, D. G., Downing, S. J. and Bradshaw, J. M. C. (1979). Relaxin inhibits spontaneous and prostaglandin-driven myometrial activity in anaesthetized rats. *J. Endocrinol.* **83**, 183-192. doi:10.1677/joe.0.0830183

Potts, D. M. and Wilson, I. B. (1967). The preimplantation conceptus of the mouse at 90 hours post coitum. *J. Anat.* **102**, 1-11.

Psychoyos, A. (1961). Perméabilité capillaire et décidualisation utérine. *C R Acad. Sci.* **252**, 1515-1517.

Pusey, J., Kelly, W. A., Bradshaw, J. M. C. and Porter, D. G. (1980). Myometrial activity and the distribution of blastocysts in the uterus of the rat: interference by relaxin. *Biol. Reprod.* **23**, 394-397. doi:10.1095/biolreprod23.2.394

Restall, B. J. and Bindon, B. M. (1971). The timing and variation of pre-implantation events in the mouse. *J. Reprod. Fertil.* **24**, 423-426. doi:10.1530/jrf.0.0240423

Rogers, P. A. W., Murphy, C. R., Squires, K. R. and MacLennan, A. H. (1983). Effects of relaxin on the intrauterine distribution and antimesometrial positioning and orientation of rat blastocysts before implantation. *J. Reprod. Fertil.* **68**, 431-435. doi:10.1530/jrf.0.0680431

Salleh, N., Baines, D. L., Naftalin, R. J. and Milligan, S. R. (2005). The Hormonal Control of Uterine Luminal Fluid Secretion and Absorption. *J. Membr. Biol.* **206**, 17-28. doi:10.1007/s00232-005-0770-7

Sheng, X., Yung, Y. C., Chen, A. and Chun, J. (2015). Lysophosphatidic acid signalling in development. *Development* **142**, 1390-1395. doi:10.1242/dev.121723

Sittmann, K. (1973). Intrauterine migration of pig embryos in litters without losses. *Can. J. Anim. Sci.* **53**, 71-74. doi:10.4141/cjas73-010

Song, H., Lim, H., Paria, B. C., Matsumoto, H., Swift, L. L., Morrow, J., Bonventre, J. V. and Dey, S. K. (2002). Cytosolic phospholipase A2alpha is crucial [correction of A2alpha deficiency is crucial] for 'on-time' embryo implantation that directs subsequent development. *Development* **129**, 2879-2889.

Tsutsui, T., Amano, T., Shimizu, T., Murao, I. and Stabenfeldt, G. H. (1989). Evidence for transuterine migration of embryos in the domestic cat. *Jpn. J. Vet. Sci.* **51**, 613-617. doi:10.1292/jvms1939.51.613

Tsutsui, T., Shimizu, T., Hori, T. and Kawakami, E. (2002). Factors affecting transuterine migration of canine embryos. *J. Vet. Med. Sci.* **64**, 1117-1121. doi:10.1292/jvms.64.1117

Vasquez, Y. M., Wang, X., Wetendorf, M., Franco, H. L., Mo, Q., Wang, T., Lanz, R. B., Young, S. L., Lessey, B. A., Spencer, T. E. et al. (2018). FOXO1 regulates uterine epithelial integrity and progesterone receptor expression critical for embryo implantation. *PLoS Genet.* **14**, e1007787. doi:10.1371/journal.pgen.1007787

Wilson, I. B. (1962). Mechanisms of implantation of the ovum. *Carnegie Instn Wash. Yb.* **61**, 421.

Ye, X., Hama, K., Contos, J. J. A., Anliker, B., Inoue, A., Skinner, M. K., Suzuki, H., Amano, T., Kennedy, G., Arai, H. et al. (2005). LPA3-mediated lysophosphatidic acid signalling in embryo implantation and spacing. *Nature* **435**, 104-108. doi:10.1038/nature03505

Yoshinaga, K., Rice, C., Krenn, J. and Pilot, R. L. (1979). Effects of nicotine on early pregnancy in the rat. *Biol. Reprod.* **20**, 294-303. doi:10.1095/biolreprod20.2.294

DEVELOPMENT